Optical properties of amorphous SiO_2-TiO_2 multi-nanolayered coatings for 1064-nm mirror technology

Optical properties of amorphous SiO_2-TiO_2 multi-nanolayered coatings for 1064-nm mirror technology

M. Magnozzi[a], S. Terreni[a], L. Anghinolfi[a], S. Uttiya[a], M.M. Carnasciali[b], G. Gemme[c], M. Neri[a,c], M. Principe[d], I. Pinto[d], L.-C. Kuo[e], S. Chao[e], M. Canepa[a,c,*]

[a] *OPTMAT Lab, Dipartimento di Fisica, Università di Genova, via Dodecaneso 33, 16146 Genova, Italy*
[b] *Dipartimento di Chimica e Chimica Industriale, Università di Genova, via Dodecaneso 31 I-16145 Genova, Italy*
[c] *Istituto Nazionale di Fisica Nucleare, Sezione di Genova, via Dodecaneso 33, 16146 Genova, Italy*
[d] *Dept. of Engineering, University of Sannio, C.so Garibaldi 107, I-82100 Benevento, Italy*
[e] *Institute of Photonics Technologies & E.E. Dept., National Tsing Hua University 101 Kuangfu Rd. Sec. 2 Hsinchu, Taiwan 300*

Abstract

The use of amorphous, SiO_2-TiO_2 nanolayered coatings has been proposed recently for the mirrors of 3^{rd}-generation interferometric detectors of gravitational waves, to be operated at low temperature. Coatings with a high number of low-high index sub-units pairs with nanoscale thickness were found to preserve the amorphous structure for high annealing temperatures, a key factor to improve the mechanical quality of the mirrors. The optimization of mirror designs based on such coatings requires a detailed knowledge of the optical properties of sub-units at the nm-thick scale. To this aim we have performed a Spectroscopic Ellipsometry (SE) study of amorphous SiO_2-TiO_2 nanolayered films deposited on Si wafers by Ion Beam Sputtering (IBS). We have analyzed films that are composed of 5 and 19 nanolayers (NL_5 and NL_{19} samples) and have total optical thickness nominally equivalent to a quarter of wavelength at 1064 nm. A set of reference optical properties for the constituent materials was obtained by the analysis of thicker SiO_2 and TiO_2 homogeneous films ($\sim$ 120 nm) deposited by the same IBS facility. By flanking SE with ancillary techniques, such as TEM and AFM, we built optical models that allowed us to retrieve the broad-band (250-1700 nm) optical properties of the nanolayers in the NL_5 and NL_{19} composite films. In the models which provided the best agreement between simulation and data, the thickness of each sub-unit was fitted within rather narrow bounds determined by the analysis of TEM measurements on witness samples. Regarding the NL_5 sample, with thickness of 19.9 nm and 27.1 nm for SiO_2 and TiO_2 sub-units, respectively, the optical properties presented limited variations with respect to the thin film counterparts. For the NL_{19} sample, which is composed of ultrathin sub-units (4.4 nm and 8.4 nm for SiO_2 and TiO_2, respectively) we observed a significant decrease of the IR refraction index for both types of sub-units; this points to a lesser mass density with respect to the thin film reference. The results are discussed in the light of the existing literature on nanofilms of amorphous oxides.

Keywords: Spectroscopic ellipsometry, coatings, multilayer, SiO_2 thin film, TiO_2 thin film.

*Corresponding author

1. Introduction

The first, direct observations of gravitational waves (GW) [1, 2, 3] has crowned with success decades of research on detectors (GWD) based on long-baseline Fabry-Perot interferometers. On the other hand a definite improvement of sensitivity is even more desirable to optimize the performance of GWD in future, 3^{rd}-generation experiments.
The dominant noise source impacting the performances of the present GWDs, which lies in the range between a few tens and a few hundred Hz, has been identified in the thermal noise of the multilayer coating of the interferometer mirrors [4, 5, 6]. These coatings are currently composed of alternating layers of low and high refractive index glassy oxides, namely Ti-doped Ta_2O_5 and SiO_2, and are designed to have the maximum reflectivity at the wavelength of the GWD laser, that is 1064 nm [7]; the constituent materials were selected to achieve the lowest optical and mechanical losses (and hence the lowest noise, on account of the fluctuation-dissipation theorem). Efforts are underway to further optimize this design [8]. At the same time new materials and new coating designs are under active scrutiny [9, 10]. Promising developments regard crystalline semiconductor materials, Si samples [11] or MBE-grown III-V multilayer coatings on Si [12, 13], which are endowed with extremely low mechanical losses and high reflectivity.

In order to reduce thermal noise, 3^{rd}-generation GWD will operate at cryogenic temperatures [14]. However, the Ta_2O_5 sub-units of the coatings presently in use are significantly affected by low-temperature mechanical losses [15]. TiO_2 is an appealing high-index material substitute, featuring low mehanical losses down to a few K. On the other hand, it is prone to cystallization (which spoils both its optical and mechanical qualities) upon post-deposition annealing. This occurs in a thickness dependent way: thinner and thinner TiO_2 layers tolerate higher temperatures without crystallization [16]. A nanolayered structure has been proposed recently consisting of a stack of several pairs of SiO_2-TiO_2 sub-units [17, 18, 19]. By adjusting the SiO_2/TiO_2 volume ratio, the stack can be designed to obtain a fine tuning of refractive index, and can be profitably used as a "metamaterial" substitute for the Ta_2O_5-based material presently in use. Recent checks on the nanolayered films confirm the absence of definite peaks in mechanical losses measurements at cryogenic temperatures [20].

Due to physical reasons and for fine aspects related to the growth modalities [21, 22, 23] the optical properties of sub-units at the very nanoscale thickness may be significantly different from those of of customary optical films, with typical thickness $\sim$ 100 nm, and from those of the bulk materials. In order to optimize the design of mirrors employing the composite nanolayers technology it is therefore necessary to quantify these differences, under the conditions of fabrication typical of these particular multilayers.

This paper is focused on the optical characterization of nanolayered SiO_2-TiO_2 films deposited on silicon wafers by ion beam sputtering [17], performed by Spectroscopic Ellipsometry (SE). The SE measurements have been performed from UV to NIR (250-1700 nm), thus covering a wide spectral region encompassing the wavelength of 1064 nm presently used in GWD (including also 1550 nm proposed for future GWD detectors). All tested prototypes were designed to have the same nominal effective refraction index, and the same optical thickness (one quarter of wavelength at $1064nm$). Our main aim was to address the case of nanolayer film prototypes with 19 sub-units, denoted for brevity NL_{19}, that tolerated annealing at relatively high temperature without showing crystallization [17] and could be accordingly a high-index material candidate for the GWD mirror coatings.

The SE analysis presented two challenging issues related to the sub-units composing the coatings: their ultrathin thickness (a few nm) and their rather high number. The interlacing of these two aspects entails subtle correlations among the SE fitting parameters, i.e. the actual thickness and refractive index of the nanolayers. Previous SE experiments of SiO_2-TiO_2 multilayers with "thin" sub-units provided a useful database [24, 25]. However, we also needed reference values for SiO_2 and TiO_2 films grown under the same (fiducial) conditions adopted for the multi-nanolayered composite films. In this respect, two films of SiO_2 and TiO_2, about 120 nm thick, provided the necessary reference. In addition, ancillary to the analysis of the NL_{19} sample, we also considered another quarter-wave multilayer with five sub-units, denoted as NL_5. For this sample the SE analysis is simpler as sub-units are a few tens of nm thick. The NL_5 coating showed crystallization after annealing and hence it is not suitable for GWD mirror fabrication; nevertheless it proved useful in the perspective of this work, since it represented an intermediate system between the thin-film reference case and the thinnest (nm-scale) nanolayers of NL_{19}.
Our estimate of the broad-band optical properties of the multilayer coatings relies on two basic ingredients: first, the use of TEM on witness samples to obtain independent measurements of sub-units thickness and of AFM to check surface roughness; second, the use of viable approximations introduced in the optical models which represent the sub-units.

Our analysis points to the fact that optical properties of sub-units with nanoscale thickness are significantly different from those of the thin films and bulk materials references. An extended discussion of existing literature will help to rationalise these findings, which represent a useful feedback for the design and fabrication of the multilayer mirrors. To our knowledge, this is the first time that a SE analysis of a multilayer coating with a high number of ultrathin sub-units is attempted. Beyond their importance for 3^{rd}-generation GWD mirrors, the nanolayered systems analyzed in this work offer the opportunity to study the optical properties of highly uniform layers of materials which are strategic in many

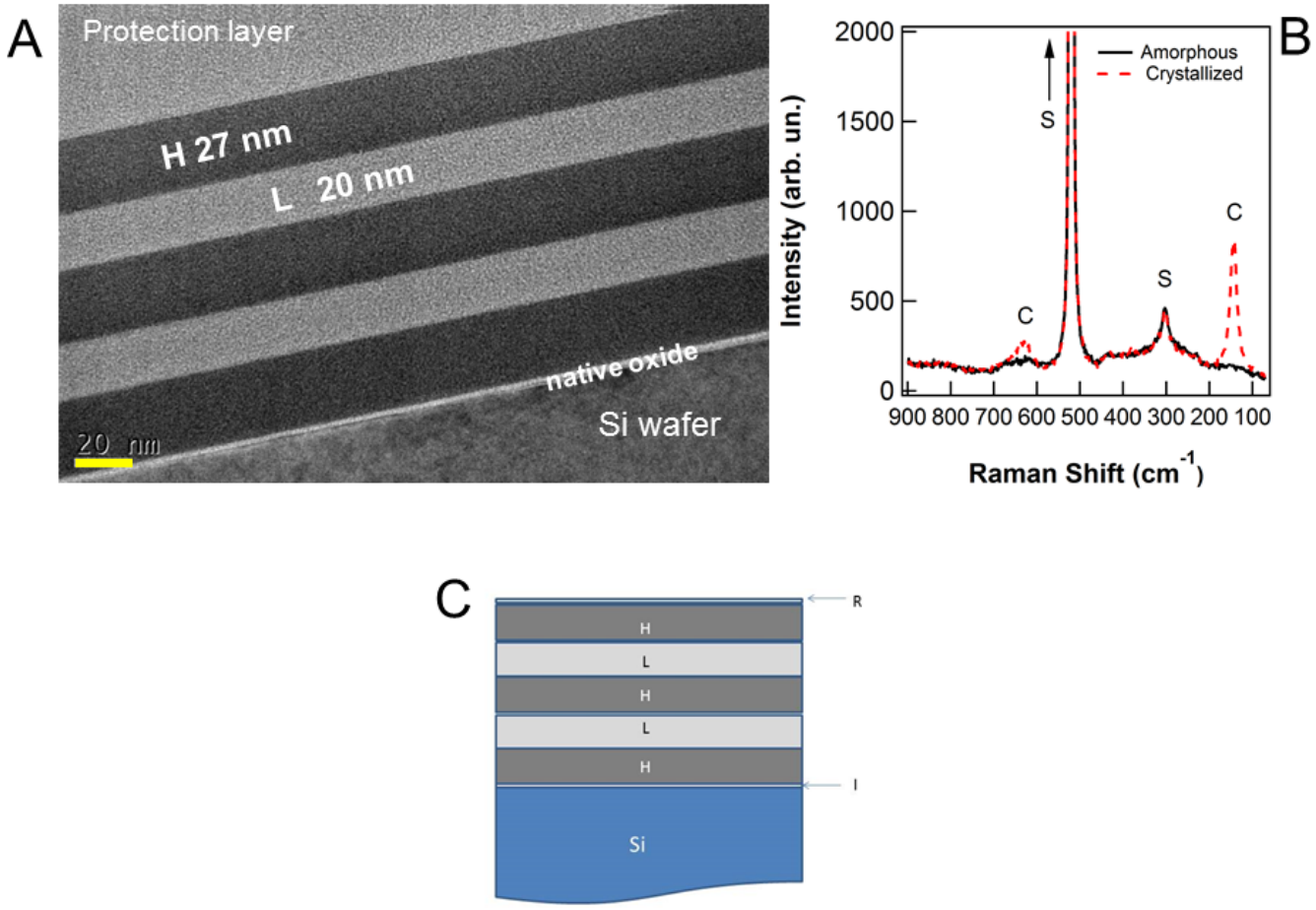

Figure 1: (A) TEM image of the NL_5 coating (witness sample with protection layer). The protection layer is not present in the samples used for ellipsometry measurements. (B) Representative Raman spectra of the NL_5 coating. S = substrate peaks. The spectra emphasize the difference between the as-deposited amorphous film (black line) and the film annealed to 300 °C (dotted line) which shows peaks related to the crystalline phase (C peaks) . (C) structure of the optical model used for the analysis of the multilayer samples, on the example of NL_5 . From bottom to top: Silicon substrate (Si), Native Oxide (I), TiO_2/SiO_2 layers (H/L), and surface roughness (R).

technological contexts, at the nanoscale and under the particular "sandwiched" conditions typical of multilayer coatings.

2. Materials and Methods

The coatings were deposited by Ion Beam Sputtering on 1x4 cm^2 substrates, which were cut from a one-side polished Si wafer (Ø 4", thickness 525±25 μm, surface roughness 0.15±0.02 nm, orientation (100), p-type with B-doping concentration of $10^{16}/cm^3$, resistivity ~1-10 Ohm cm) covered by native oxide. After the deposition, the central area of the wafer was cut into 3 pieces, each 1x1 cm^2. In each coating, the deepest sub-unit composed of TiO_2 is covered by a number of SiO_2-TiO_2 pairs; the sub-unit at the top of the stack is TiO_2. Witness samples, coated with a SiO_2 protection layer, were used for TEM measurements [17]. The actual thickness of the SiO_2 and TiO_2 sub-units as measured by TEM were respectively 19.9 nm and 27.1 nm for NL_5, and 4.4 nm and 8.4 nm for NL_{19}. The structure of the NL_5 coating is shown in Fig. 1. *H* and *L* denote *high-index* (TiO_2) and *low-index* (SiO_2) sub-units.
SE measurements on un-annealed, as-deposited samples have been performed with a J.A. Woollam M-2000 spectroscopic ellipsometer (674 points in the 250-1700 nm spectral range), at room temperature in free air, at three angles of incidence (60° - 65° - 70°). The size of the beam spot measures several mm^2. For the data analysis we used the WVASE software; we looked for the best agreement between the experimental and calculated (Ψ, Δ)-spectra by running an algorithm that

minimizes the Mean Squared Error (MSE) function defined as [26]:

$$\mathrm{MSE} = \sqrt{A \cdot \sum_{i=1}^{N} \left[\left(\frac{\Psi_i^{exp} - \Psi_i^{calc}}{\sigma_{\Psi,i}^{exp}} \right)^2 + \left(\frac{\Delta_i^{exp} - \Delta_i^{calc}}{\sigma_{\Delta,i}^{exp}} \right)^2 \right]}$$

where $\sigma_{\Psi,i}^{exp}$ and $\sigma_{\Delta,i}^{exp}$ are the standard deviations of the acquired Ψ and Δ. The parameter A is defined as:

$$A = \frac{1}{2L - M}$$

where L is the number of points, and M is the number of fitted parameters.

The analysis of the SE spectra of the multilayer samples involved precursor steps. First, we characterized the bare substrate (Si covered by native SiO_2); then, we considered two samples coated with SiO_2 and TiO_2 thin monolayer films, for reference; finally, we built an optical model for multi-nanolayered samples, addressing sequentially the NL_5 and NL_{19} samples. In such model, the parameters of the substrate were fixed to the results of first step, and the parameters of the SiO_2 and TiO_2 sub-units were fitted to the experimental data by using the results obtained on the reference thin films as the starting point.

We tried different models to check the dependence of the results on the choice of the model structure, and we checked for possible sample non-idealities (such as a limited thickness non-uniformity) to evaluate the influence of such characteristics on the fit results.

The SE measurements were flanked by TEM and AFM with the aim of obtaining independent information about the sub-units thickness and surface roughness, respectively. Raman spectroscopy measurements were used to check the sub-units phase (amorphous or crystalline). Representative TEM and Raman measurements are reported in Fig. 1.

3. Data analysis

3.1. Substrate

The substrate was modelled as a two-layer stack, representing Si (bottom) and native SiO_2 (top). For SiO_2 we used tabulated data [27], while for Si we used a parametrized model with six oscillators (so-called Parametric-Si model in WVASE). Our approximation of flat surface for this model was validated by AFM measurements, which indicated a surface roughness less than 0.2 nm. The agreement between simulated and the experimental data (not shown here) was satisfactory (MSE = 2.4); the calculated SiO_2 thickness, about 2 nm, was in line with expectations for native oxide and consistent with TEM measurements.

3.2. Monolayer films

These films have been modelled as a stack of four layers: the Si substrate, the native SiO_2 layer, the deposited layer (SiO_2 or TiO_2) and the surface layer. The optical properties of substrate and native oxide layer resulted from the analysis of the uncoated samples. The surface layer, for simplicity, was modelled through the well-known *roughness* layer, a Bruggeman Effective Medium Approximation (B-EMA) model with 50-50 % fractions of coating and so-called voids [28, 29].

3.2.1. SiO_2 films

Library data for the SiO_2 optical properties gave only qualitative agreement with the measurements (MSE $\approx 60-70$). We opted for parametric models commonly used for transparent layers. Models such as the Cauchy or the Two-Pole model gave closely similar outcomes. In the Cauchy model the refractive index was calculated as $n(\lambda) = A + B/\lambda^2 + C/\lambda^4$ and the extinction coefficient was set to zero. The three parameters A, B and C along with the thickness of the SiO_2 film were set as adjustable parameters. Main fit results for this sample are reported in Table 1. As can be seen in Fig. 2-A, the fitting procedure resulted in a good agreement with the data (MSE=12.0). The resulting thickness of the SiO_2 layer was 126.5 nm, a value that is compatible with the estimate of 129 ± 1 nm derived by TEM for the sum of the coating thickness plus the native oxide thickness. The inclusion of the roughness layer had negligible influence on the fit quality and optical properties of the films and, for this reason, it was abandoned. The calculated value of the refractive index n at 1064 nm was 1.480.

We also tested the Cauchy – Urbach model, that complements the Cauchy interpolation formula with an extinction coefficient which exponentially decays with λ. Fit improvements were negligible and the calculated absorptions, below the experimental sensitivity (less than 10^{-3}), were regarded as fictitious. The thickness non-uniformity for this sample

was "rejected" by the fit algorithm (i.e., its calculated value was 0.0%). The Two-Pole model provided fit values very close to those obtained with the Cauchy model (MSE = 13.2; n@1064 nm = 1.479).

From our analysis, we concluded that the uncertainty on the value of the refractive index for the SiO_2 reference thin film in the IR range was in the order of 10^{-3}.

3.2.2. TiO_2 films

The optical properties of the TiO_2 layer were modelled using the Cody-Lorentz (CL) expression in the Kramers-Krönig-consistent form proposed in Ref.[30], which is often used to model the profile of the fundamental absorption threshold of amorphous, wide-gap semiconductors [31, 32, 33, 34]. The CL formula provides a parametrized expression for the imaginary part of the dielectric function (ε_2) by analysing the "deviations" of the electronic structure of the amorphous material from the crystalline state, and "partitioning" the photon energy range around the absorption threshold into three analytically connected regions: below, across, and above the optical gap. Below the gap the ε_2 has the shape of an Urbach-like exponential adsorption tail [35]; at photon energies slightly greater than E_g, the model assumes that $\varepsilon_2 \propto (E - E_g)^2$; while well above the gap, the model includes a Lorentzian oscillator.

By fitting the model to the data, we obtained the results reported in Fig. 2-B and Table 1. The MSE (16.5) was somewhat higher than in the case of the SiO_2 monolayer sample. The estimated thickness of the film and roughness layer were 119.3 and 1.6 nm, respectively, compatible with the values of 121 ± 1 based on TEM measurements and with AFM roughness of around 2 nm. If the spectral range of our analysis is confined to the transparent region (400-1700 nm) the agreement with the data improves, MSE=11.7, with tiny impact over the resulting n of TiO_2 in the IR range. These findings would suggest to assign at least part of the disagreement between data and simulations in the full range to some inadequacies of the CL model in the deep UV range. We checked the alternative model proposed by Bundesmann and coworkers [36], who used two Tauc-Lorentz oscillators to describe the absorption region; however, we always obtained results very close to those presented in Tab. 1, without any clear fit improvement. Attempts to improve the quality of this fit by including non-idealities (such as thickness non-uniformity, vertical grading and intermixing between native SiO_2 and TiO_2) also proved unfruitful.

3.3. Multilayer coatings

The fitting of SE data of multilayer coatings independently from TEM values provided the order of magnitude for the sub-unit thickness. However, correlations between parameters prevented us from obtaining simultaneous, accurate information on the sub-units thickness and optical properties for both TiO_2 and SiO_2 materials.
In order to soften the impact of parameter cross-correlation, we used the simplest structure for our models by imposing the same optical properties for sub-units of the same material, thus reducing considerably the parameters to be fitted. After examination of TEM images we also assumed sharp interfaces between the sub-units.

As a first attempt, for both types of coating examined, the optical properties of SiO_2 and TiO_2 sub-units were set to the reference values obtained for the monolayer films. The thickness of each sub-unit was set to the value obtained from the analysis of TEM images, leaving as free parameter only the surface roughness layer thickness. For this basic model the agreement with the experimental data was not satisfactory (MSE=76.5 and 332 for the NL_5 and NL_{19} samples, respectively). We then moved to models of increasing flexibility that are described hereafter.

3.3.1. NL_5 coating

In a second model, the thickness of each sub-unit was left free to vary within the range of uncertainty of the TEM measurements ($\pm$0.25 nm), still assuming the thin film optical properties. The fit to the data showed a limited improvement (MSE = 42.5). The discrepancy between data and simulations had therefore to be in part associated to difference of the optical properties of the sub-units with respect to the corresponding monolayers reference.

In order to clarify this point, we admitted fit adjustments of the optical parameters of the two materials, while the thickness of each sub-unit was set to the value provided by TEM. In this case the MSE improved to 20.3. The low value of the roughness layer thickness, 0.9 nm, was in good consistence with AFM. Both the TiO_2 and SiO_2 optical properties showed variations with respect to the thin film references. The TiO_2 energy gap moved from 3.165 to 3.145 eV; however the IR refractive index presented only a very limited change (from 2.320 to 2.318 at 1064 nm). The n@1064 nm of SiO_2 passed from 1.48 to 1.51. Conceivable non-idealities, such as a small thickness non-uniformity, did not provide any clear improvement to the agreement with the experimental data and had a negligible impact on the calculated parameters such as the refractive index and energy gap.

Finally, in a last refinement of the model, the thickness of each sub-unit was again left free to vary within the range of uncertainty of the TEM measurements ($\pm$0.25 nm). The MSE showed a residual improvement from 20.9 to 18.8. The comparison between these best-fit simulations and data is shown in Fig. 2-C. The optical parameters of TiO_2, as well as the surface roughness, remained substantially unaltered with respect to the results of the previous model, while a

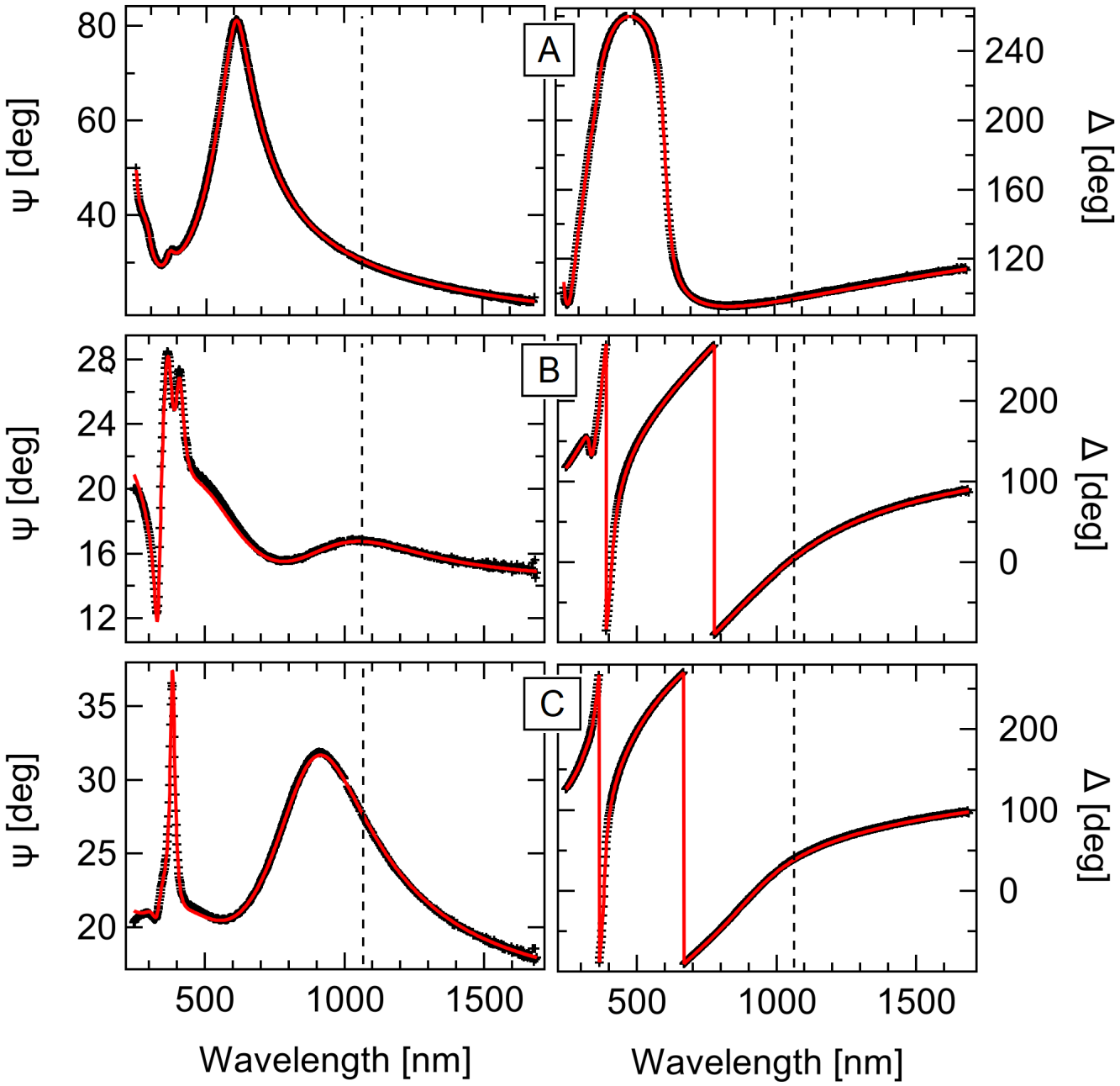

Figure 2: Ellipsometry spectra (markers, black) and best-fit simulations (lines,red). A: SiO_2 thin film; B: TiO_2 thin film; C: NL_5 multilayer coating. See text for the description of employed models. The dotted vertical line in all panels indicates the 1064-nm wavelength.

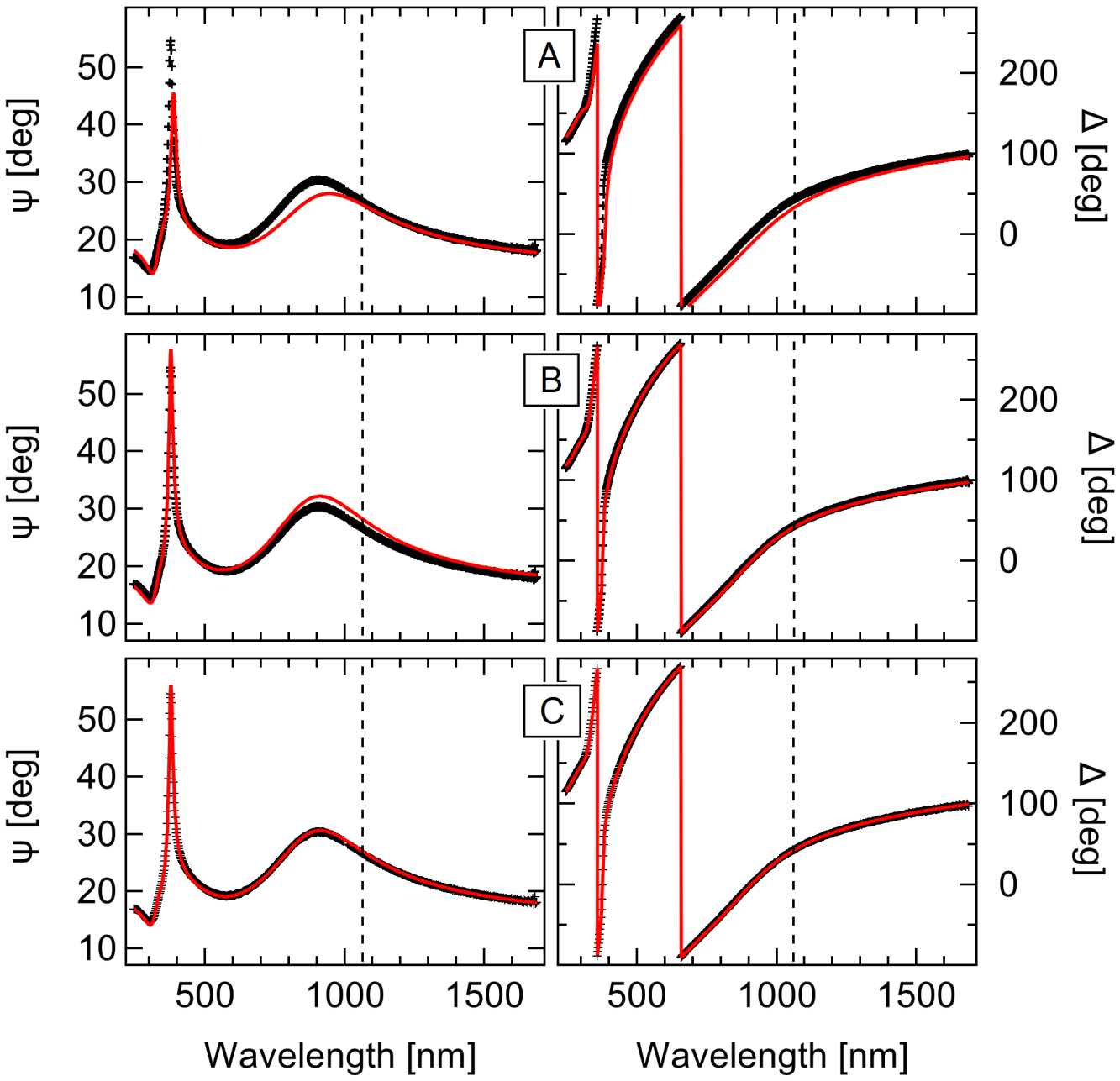

Figure 3: Ellipsometry spectra (markers, black) and simulations (lines, red) for the NL_{19} multilayer coating. A: the thickness of each sub-unit was set to the TEM value, and the optical properties of TiO_2 and SiO_2 were those retrieved from the NL_5 coating. The thickness of the roughness layer was the only fit parameter (MSE = 320). B: as in A but the optical properties of TiO_2 and SiO_2 were fitted (MSE=29.4). C: Best-fit model. As in B but the thickness of each layer was fitted within the TEM experimental uncertainty (MSE = 16.0).

Sample	Free Parameters	n@1064 nm	MSE
SiO_2 thin film	SiO_2 thickness SiO_2 Cauchy parameters	1.480	12.0
TiO_2 thin film	TiO_2 thickness TiO_2 CL parameters	2.320	16.5
NL_5 multilayer	surface roughness SiO_2 Cauchy parameters TiO_2 CL parameters sub-units thickness*	1.50 (SiO_2) 2.32 (TiO_2)	18.8
NL_{19} multilayer	surface roughness SiO_2 Cauchy parameters TiO_2 CL parameters sub-units thickness*	1.41 (SiO_2) 2.28 (TiO_2)	16.0

Table 1: Fit results of the SE spectra for the SiO_2 and TiO_2 thin films and multilayers. For each sample, only the results of the best-fitting model are reported; other models are discussed in the text.* fitted within the TEM uncertainty.

slight decrease of the refractive index of SiO_2 was noted, with n@1064 nm from 1.51 to 1.50 (see Table 1). The optical properties (n and κ) resulting from the best fit are shown in Fig. 4, compared with thin film reference.

3.3.2. NL_{19} coating

First we note that the fit to data did not improve significantly (MSE = 320) by substituting the reference optical properties with those retrieved from the NL_5 coating. Discrepancies between simulations and data can be appreciated in Fig. 3-A, most notably for Ψ data. Maintaining the reference optical properties and fitting the thickness of each layer within the TEM experimental uncertainty the agreement showed only a limited improvement (MSE = 155). Thus we allowed the optical properties of TiO_2 and SiO_2 to be fitted, and the agreement with data significantly improved (MSE = 29.4), as it can be appreciated in Fig. 3-B. However the fit was still not satisfactory, especially in the region between 800 and 1200 nm. Finally, we fitted the optical properties of TiO_2 and SiO_2 as well as the thickness of each sub-unit, within the TEM experimental uncertainty; a definite improvement of the MSE (16.0) was obtained as it is shown in Fig. 3-C. The surface roughness layer thickness was 0.9 nm, compatible with AFM measurements. Looking at the calculated optical properties of TiO_2 and SiO_2, reported in Fig. 4, we noticed clear variations with respect to the monolayer reference (see also Table 1), most notably for SiO_2, for which we found $n = 1.41$ at 1064 nm. The energy gap of TiO_2 shifted to $E_g = 3.21$ eV and n at 1064 was nm =2.28. The optical properties (n and κ) resulting from the best fit are reported in Fig. 4. We point out that the inclusion of non-idealities in the model resulted in a slightly better agreement (with 5% thickness non-uniformity, MSE=13.7) without implying significant variations of the optical properties. Also the surface roughness remained unaltered at 0.9 nm.

4. Discussion and concluding remarks

Our analysis of SE data on multi-nanolayered amorphous coatings relies on two basic ingredients: (i) a characterizationof amorphous SiO_2 and TiO_2 thin films deposited under similar growth conditions and (ii) the ancillary analysis of TEM and AFM measurements on witness samples.

The determination of reference optical properties carried out on coatings about 120-130 nm thick clearly played a pivotal role. For these samples, viable optical models (i.e. the Two-Poles or Cauchy models for SiO_2 and the Cody-Lorenz model for TiO_2) reproduced accurately broadband SE data with some disagreements limited to the deep UV range, and provided the IR refractive index with an uncertainty in the order of 10^{-3}. The thickness of thin films determined by ellipsometry was fully consistent with the values derived from TEM measurements obtained on witness samples.

The reference optical properties of the thin films, reported in Fig. 4, were consistent with the literature reporting on similar samples. Regarding SiO_2, the dispersion of n (top panel, red line in Fig. 4) is fully compatible with many reports for silica films produced by IBS methods [25, 37, 38, 39, 40]. The refractive index values are relatively high and indicate a relatively dense layer [41, 42]. Regarding amorphous TiO_2, it is clear from the literature that the optical properties depend on the microstructure and morphology of films, which are in turn influenced by the growth method, growth parameters and post-deposition treatments [28, 43, 44, 45, 46, 47, 48, 49, 50, 51, 52, 53, 54]. Though a tight comparison of our results with the literature is not straightforward, we note that the optical gap found here for thin

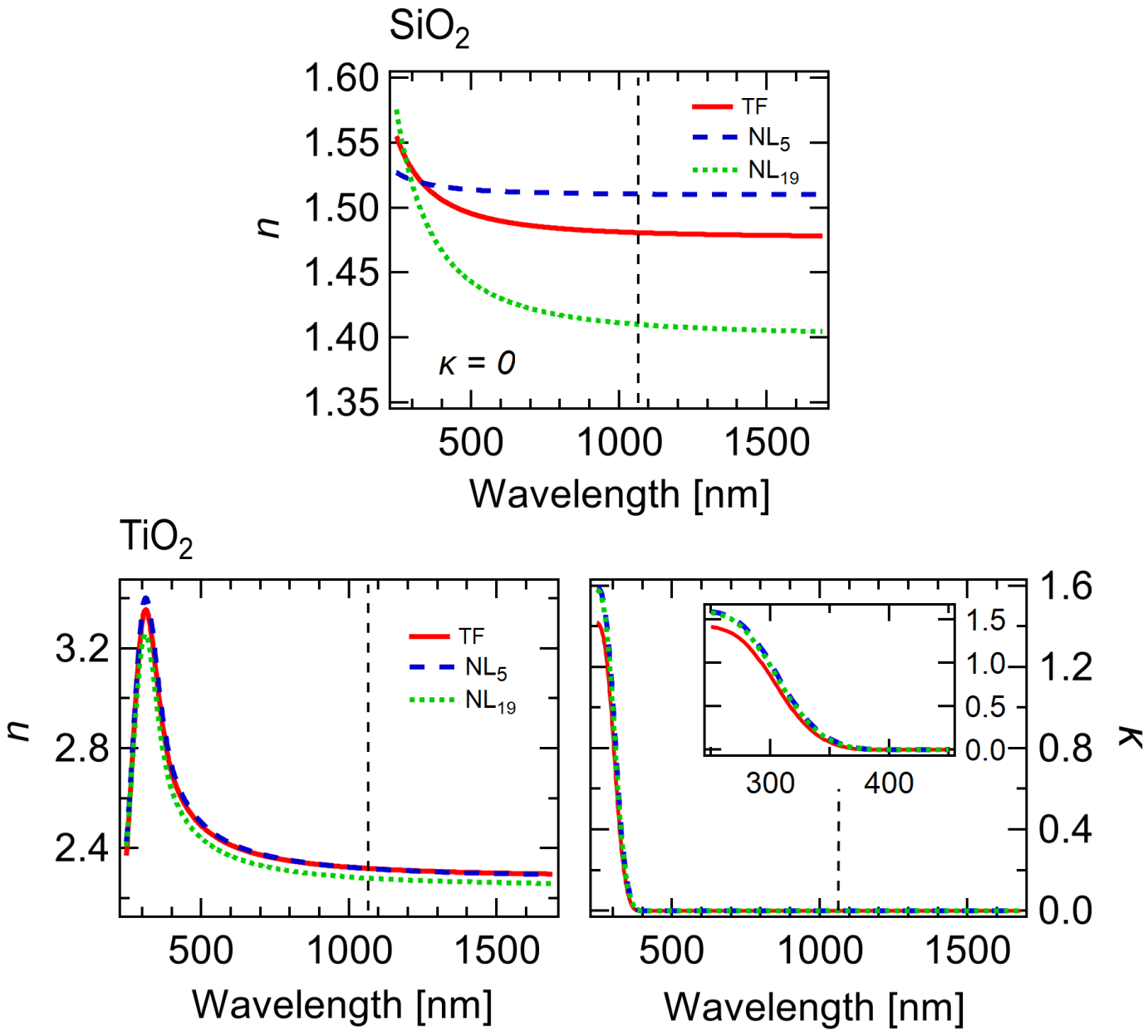

Figure 4: Calculated optical properties for SiO_2 and TiO_2 monolayer thin films (TF), 5-layer coating (NL_5) and 19-layer coating (NL_{19}). Top: calculated SiO_2 refractive index Bottom: calculated TiO_2 refractive index and extinction coefficient.The dotted vertical line in all graphs indicates the 1064-nm wavelength.

films is slightly smaller than the values (in the range 3.2-3.3) reported for high-density films [36, 49, 55, 56, 57]. Many articles in the literature comment on the value of the refractive index of TiO_2 at 550 nm. Values of n at 550 nm in the 2.4-2.5 range were reported in recent [36] as well as early works [58, 46], for coatings produced by several types of ion beam sputtering methods. The values we found at 550 nm, around 2.44, are fully compatible with the literature values reported for ion-beam sputtered TiO_2 films. Other works reported higher values, e.g in the 2.50-2.56 range [57, 59, 60] or lower values, in the 2-2.3 range, for film obtained by evaporation methods [49]. Several groups have commented about the correlation of the index of refraction with the coating density, applying the Clausius-Mossotti or Lorentz-Lorenz equations [46, 49, 60, 61]. This aspect was thoroughly reviewed by Bundesmann and coworkers [36]; according to data reported in Fig. 11 of Ref.[36], the density of our film should be estimated ~ 3.5 g/cm^3. Having compared our results with the existing literature, we could be confident on a set of reference optical properties to be employed for the analysis of nanolayered coatings with decreasing sub-units thickness.

While for thin films TEM was used *a posteriori* as a useful check of the SE analysis results, for the multilayers TEM measurements fed the SE analysis *a priori* by (i) helping to introduce viable simplifications in the optical models and (ii) setting reference values and proper uncertainty limits for the thickness of sub-units. TEM thus provided an effective means to "solve" physical and mathematical correlation issues among thickness and optical parameters in the fit procedures. Based on modelling steps of increasing complexity, the analysis showed that the optical properties of TiO_2 and SiO_2 in the multilayer coatings are different from the thin film reference, as it is shown Fig.4.

Differences appear relatively small in the case of NL_5, whose sub-units are still relatively thick (few tens of nanometres). The optical properties of the TiO_2 sub-units showed a *slight* deviation from the thin-film reference values only in the absorption threshold region (in the UV range), while IR properties were practically unchanged. For SiO_2 sub-units, instead, the fit provided a change of dispersion with an IR increase of about 2%, larger than the model uncertainty of 1%. This finding appears consistent with the results of previous works which studied the optical properties of SiO_2 as a function of decreasing thickness [22, 23]. Ref.[22] reported a few % increase of refractive index going from 160 nm down to 20 nm film thickness. Cai et al.[23] reported a slight increase of the refractive index for thickness in the 60-10 nm range while films thicker than 60 nm showed values close to bulk SiO_2. Refs.[22, 23] assign the effect to compressive stress.

For the NL_{19} multilayer coating, whose sub-units thickness falls below 10 nm, we found appreciable deviations of the optical properties from the thin film references. In particular we observed a decrease of the IR index for both types of sub-units, as reported in Fig.4.

For the TiO_2 sub-units, the complex refractive index values can be compared with those recently obtained in ref.[62] for films with thickness in the 2-20 nm range. An overall decrease of the refractive index for decreasing thickness was observed in that work; our data are compatible with this finding as we noticed an analogous trend going from the NL_5 to the NL_{19} coating - that is, by reducing the thickness of the TiO_2 sub-units (see Fig. 4, bottom). Such trend was assigned by Shi et al. to a density variation which is due to the increased percentage of volume occupied by voids that occurs when the film thickness is reduced [62].

Concerning the ultrathin SiO_2 films (thickness $<$10 nm), the literature shows diverse trends. Refs.[63] and [21] reported an increase of n when decreasing the thickness from 8 to 2 nm. Ayupov et al. [64], on the other hand, observed an overall constant value of n for thickness in a similar thickness range. The already mentioned paper by Cai et al.[23] provides hints to explain these apparently contradictory findings, by indicating a correlation between the refractive index and the processing conditions that affect the film morphology. The trend reported by Refs.[63] and [21] was obtained also by Cai et al. for slow growth rates. Faster deposition rates induced a more granular morphology, resulting in a sharp drop of the refractive index for film thickness below 10 nm. In this respect, the paper reported a decrease in n from 1.48 to 1.37 at 550 nm. In our case, the AFM and TEM measurements of the NL_{19} coating did not show an evidently rough morphology; consequently, the thickness of the surface roughness layer in the SE model was rather low, below 1 nm. We note that our models, while firmly backing on TEM measurements, have been based on the assumption of sharp interfaces between sub-units. However, even a minimum amount of disorder, with possible formation of nano-voids or mixing effects at the interfaces, is expected to affect the global optical properties of a multilayer system with many interfaces such as the NL_{19} coating [65]. The presence of some amounts of voids shouldn't be excluded at the very nanoscale, also in view of our previous experiments on other amorphous oxides [32]. In this respect, we note that the last step of the SE analysis of multilayer coatings, that provided the best agreement with the data, included the fitting of the thickness of each sub-unit within bound limits set by the TEM experimental uncertainty. This passage didn't improve too much the MSE and had scarce effect on optical parameters in the case of the NL_5 coating. For this coating indeed, the relative uncertainty on TEM thickness is rather low, in the order of 1-2 %. The picture changes for the NL_{19} coating. Here, especially for the the SiO_2 units, the constraints set by TEM are less stringent. On the one hand this fact provided more flexibility in the fitting process; on the other hand the approach may mask other factors, like e.g. a limited interface disorder.

In conclusion we showed that, thanks to the information on the coating morphology coming from auxiliary methods

such as TEM, and pivoting on reliable thin-film optical references, it has been possible to apply SE to deduce important information on the optical properties of a very peculiar layered system such as NL_{19}, a multilayer coating with sub-unit thickness at the very nanoscale (<10 nm). In particular, we found that the optical properties of the sub-units are quite different from the ones in the thin-films references, especially in the case of SiO_2. We remark the role of the NL_5 system as a necessary, intermediate step in our analysis flow between the thin-film references and the nano sub-units of NL_{19}. The output of our analysis indicates that in order to improve the reliability of the analysis of SE data for multi nano-layered, amorphous oxide systems, an even better knowledge of the interface morphology would be important, which is a hard task for this type of system. However, if we intend the optical properties determined for the NL_{19} coating as a set of effective properties which include the effect of interfaces, the current status of the analysis suggests that the growth conditions for this special kind of multilayers should be optimized if optical properties more similar to reference thin film values are desirable. This is an important take home message for the film fabrication in view of eventual applications to mirror technology.

Acknowledgments

This research was supported by I.N.F.N. through the project ADCOAT. The work had also received partial support from Regione Liguria through the project SAFEMAP. Sureeporn Uttiya acknowledges a post-doctoral grant from Regione Liguria (Italy). Ministry of Science and Technology of Taiwan under the contract 100-2221-E-007-009-MY3 is acknowledged regarding the sample preparation.

Bibliography

[1] B.P. Abbott et al. Observation of Gravitational Waves from a Binary Black Hole Merger. *Phys. Rev. Lett.*, 116(6), 2016.
[2] B.P. Abbott et al. GW151226: Observation of Gravitational Waves from a 22-Solar-Mass Binary Black Hole Coalescence. *Phys. Rev. Lett.*, 116(24), 2016.
[3] B.P. Abbott et al. GW170104: Observation of a 50-Solar-Mass Binary Black Hole Coalescence at Redshift 0.2. *Phys. Rev. Lett.*, 118, 2017.
[4] S. Rowan, J. Hough, and D.R.M. Crooks. *Phys. Lett. A*, 347:25–32, 2005.
[5] GM Harry, H Armandula, E Black, DRM Crooks, G Cagnoli, J Hough, P Murray, S Reid, S Rowan, P Sneddon, MM Fejer, R Route, and SD Penn. *Appl. Optics*, 45, 2006.
[6] S. Reid and I. W. Martin. Development of Mirror Coatings for Gravitational Wave Detectors. *Coatings*, 6, 2016.
[7] L. Pinard, C. Michel, B. Sassolas, L. Balzarini, J. Degallaix, V. Dolique, R. Flaminio, D. Forest, M. Granata, B. Lagrange, N. Straniero, J. Teillon, and G. Cagnoli. Mirrors used in the LIGO interferometers for first detection of gravitational waves. *Appl. Optics*, 56, 2017.
[8] M. Granata, E. Saracco, N. Morgado, A. Cajgfinger, G. Cagnoli, J. Degallaix, V. Dolique, D. Forest, C. Franc, J.and Michel, L. Pinard, and R. Flaminio. Mechanical loss in state-of-the-art amorphous optical coatings. *Phys. Rev. D*, 93, 2016.
[9] Mitrofanov V. .P, Chao S., Pan H.-W., Kuo L.-C., Cole G., Degallaix J., and Willke B. Technology for the next gravitational wave detectors. *Sci. China Phys Mech*, 58, 2015.
[10] G. Harry, T.P. Bodiya, and R. DeSalvo, editors. *Optical coatings and thermal noise in precision measurements*. Cambridge University Press, 2012.
[11] T. Kessler, C. Hagemann, C. Grebing, T. Legero, U. Sterr, F. Riehle, M. J. Martin, L. Chen, and J. Ye. A sub-40-mHz-linewidth laser based on a silicon single-crystal optical cavity. *Nat. Photonics*, 6, 2012.
[12] G.D. Cole, M.J. Zhang, W.and Martin, J. Ye, and M. Aspelmeyer. Tenfold reduction of Brownian noise in high-reflectivity optical coatings. *Nat. Photonics*, 7, 2013.
[13] A. V. Cumming, K. Craig, I. W. Martin, R. Bassiri, L. Cunningham, M. M. Fejer, J. S. Harris, K. Haughian, D. Heinert, B. Lantz, A. C. Lin, A. S. Markosyan, R. Nawrodt, R. Route, and S. Rowan. Measurement of the mechanical loss of prototype GaP/AlGaP crystalline coatings for future gravitational wave detectors. *Classical Quant. Grav.*, 32, 2015.
[14] F. Ricci. Low temperature and gravitation wave detectors in advanced interferometers and the search for gravitational waves. In M. Bassan, editor, *Advanced Interferometers and the Search for Gravitational Waves*, chapter 14. Springer, 2014.
[15] I.W. Martin, E. Chalkley, R. Nawrodt, H. Armandula, R. Bassiri, C. Comtet, M.M. Fejer, A. Gretarsson, G. Harry, D. Heinert, J. Hough, I. MacLaren, C. Michel, J.-L. Montorio, N. Morgado, S. Penn, S. Reid, R. Route, S. Rowan, C. Schwarz, P. Seidel, W. Vodel, and A.L. Woodcraft. Comparison of the temperature dependence of the mechanical dissipation in thin films of Ta2O5 and Ta2O5 doped with TiO2. *Classical Quant. Grav.*, 26, 2009.
[16] H. Sankur and W. Gunning. Crystallization and Diffusion in Composite TiO_2-SiO_2 Thin Films. *J. Appl. Phys.*, 66, 1989.
[17] H.-W. Pan, S.-J. Wang, L.-C. Kuo, S. Chao, M. Principe, I.M. Pinto, and R. DeSalvo. Thickness-dependent crystallization on thermal anneal for titania/silica nm-layer composites deposited by ion beam sputter method. *Optics Express*, 22, 2014.
[18] S. Chao, L.-C. Kuo, S.-J. Wang, H. Pan, S.-J. Song, Y.-H. Juang, I. Pinto, and R. Desalvo. Thickness-dependent crystallization on thermal anneal for the titania/silica nano-layers deposited by ion-beam-sputter method. In *LIGO-Virgo Collaboration Meeting, Hanover, Germany, Sep.23-27, 2013*, LIGO documentation number: LIGO-G1300921.
[19] M. Principe. Reflective coating optimization for interferometric detectors of gravitational waves. *Optics Express*, 23, 2015.
[20] S. Chao. Private communication.
[21] Y. Wang and E.A. Irene. Consistent refractive index parameters for ultrathin SiO2 films. *J. Vac. Sci. Technol. B*, 18, 2000.
[22] H.Z. Massoud and H.M. Przewlocki. Effects of stress annealing in nitrogen on the index of refraction of silicon dioxide layers in metal-oxide-semiconductor devices. *J. Appl. Phys. D*, 92, 2002.

[23] Q.-Y. Cai, Y.-X. Zheng, P.-H. Mao, R.-J. Zhang, D.-X. Zhang, M.-H. Liu, and L.-Y. Chen. Evolution of optical constants of silicon dioxide on silicon from ultrathin films to thick films. *J. Phys. D*, 43, 2010.
[24] D. Bhattacharyya, N.K. Sahoo, S. Thakur, and N.C. Das. Spectroscopic ellipsometry of multilayer dielectric coatings. *Vacuum*, 60, 2001.
[25] V. Janicki, J. Sancho-Parramon, O. Stenzel, M. Lappschies, B. Goertz, C. Rickers, C. Polenzky, and U. Richter. Optical characterization of hybrid antireflective coatings using spectrophotometric and ellipsometric measurements. *Appl. Optics*, 46, 2007.
[26] J.A. Woollam, B. Johs, C.M. Herzinger, J. N. Hilfiker, R. Synowicki, and C. Bungay. *SPIE Proc.*, CR72:1, 1999.
[27] C.M. Herzinger, B. Johs, W.A. McGahan, J.A. Woollam, and W. Paulson. Ellipsometric determination of optical constants for silicon and thermally grown silicon dioxide via a multi-sample, multi-wavelength, multi-angle investigation. *J. Appl. Phys.*, 83, 1998.
[28] D. Mardare and P. Hones. Optical dispersion analysis of TiO2 thin films based on variable-angle spectroscopic ellipsometry measurements. *Mat. Sci. Eng. B - Solid*, 68, 1999.
[29] P. Eiamchai, .P Chindaudom, A. Pokaipisit, and P. Limsuwan. A spectroscopic ellipsometry study of TiO2 thin films prepared by ion-assisted electron-beam evaporation. *Curr. Appl. Phys.*, 9, 2009.
[30] A.S. Ferlauto, G.M. Ferreira, J.M. Pearce, C.R. Wronski, R.W. Collins, X.M. Deng, and G. Ganguly. Analytical model for the optical functions of amorphous semiconductors from the near-infrared to ultraviolet: Applications in thin film photovoltaics. *J. Appl. Phys.*, 92, 2002.
[31] M. Prato, A. Chincarini, G. Gemme, and M. Canepa. Gravitational waves detector mirrors: Spectroscopic ellipsometry study of Ta2O5 films on SiO2 substrates. *Thin Sol. Films*, 519, 2011.
[32] L. Anghinolfi, M. Prato, A. Chtanov, M. Gross, A. Chincarini, M. Neri, G. Gemme, and M. Canepa. Optical properties of uniform, porous, amorphous Ta2O5 coatings on silica: temperature effects. *J. Appl. Phys. D*, 46, 2013.
[33] J. Sancho-Parramon, M. Modreanu, S. Bosch, and M. Stchakovsky. Optical characterization of HfO2 by spectroscopic ellipsometry: Dispersion models and direct data inversion. *Thin Sol. Films*, 516, 2008.
[34] M. Di, E. Bersch, A.C. Diebold, S. Consiglio, R.D. Clark, GJ. Leusink, and T. Kaack. Comparison of methods to determine bandgaps of ultrathin HfO2 films using spectroscopic ellipsometry. *J. Vac. Sci. Technol. A*, 29, 2011.
[35] F. Urbach. The long-wavelength edge of photographic sensitivity and of the electronic absorption of solids. *Phys. Rev.*, 92.
[36] C. Bundesmann, T. Lautenschläger, D. Spemann, A. Finzel, E. Thelander, M. Mensing, and F. Frost. Systematic investigation of the properties of tio2 films grown by reactive ion beam sputter deposition. *Appl. Surf. Science*, 421, 2016.
[37] D. Souche, A. Brunet-Bruneau, S. Fisson, V.N. Van, G. Vuye, F. Abeles, and J. Rivory. Visible and infrared ellipsometry study of ion assisted SiO2 films. *Thin Sol. Films*, 313, 1998.
[38] A. Lefevre, L.J. Lewis, L. Martinu, and M.R. Wertheimer. Structural properties of silicon dioxide thin films densified by medium-energy particles. *Phys. Rev. B*, 64, 2001.
[39] C. Bundesmann, I-M. Eichentopf, S. Maendl, and H. Neumann. Stress relaxation and optical characterization of TiO2 and SiO2 films grown by dual ion beam deposition. *Thin Sol. Films*, 516, 2008.
[40] A. Ullah, H. Wilke, I. Memon, Y. Shen, Duc T.N., and H. Woidt, C.and Hillmer. Stress relaxation in dual ion beam sputtered Nb2O5 and SiO2 thin films: application in a Fabry-Perot filter array with 3D nanoimprinted cavities. *J. Micromech. Microeng.*, 25, 2015.
[41] H. Kakiuchida, K. Saito, and A.J. Ikushima. Refractive index, density and polarizability of silica glass with various fictive temperatures. *Jpn. J. Appl. Phys. 2*, 43, 2004.
[42] N. Kitamura, K. Fukumi, J. Nishii, and N. Ohno. Relationship between refractive index and density of synthetic silica glasses. *J. Appl. Phys.*, 101, 2007.
[43] J.M. Bennett, E. Pelletier, G. Albrand, J.P. Borgogno, B. Lazarides, C.K. Carniglia, R.A. Schmell, T.H. Allen, T. Tuttlehart, K.H. Guenther, and A. Saxer. Comparison og the properties of titanium-dioxide films prepared by various techniques. *Appl. Optics*, 28, 1989.
[44] M.H. Suhail, G.M. Rao, and S. Mohan. DC reactive magnetron sputtering of titanium-structural and optical characterization of TiO2 films. *J. Appl. Phys.*, 71, 1992.
[45] L.-J. Meng and M. Pereira dos Santos. Investigations of titanium oxide films deposited by d.c. reactive magnetron sputtering in different sputtering pressures. *Thin Sol.Films*, 226, 1993.
[46] M. Laube, F. Rauch, C. Ottermann, O. Anderson, and K. Bange. Density of thin TiO2 films. *Nucl. Instr. Meth. B*, 113, 1996.
[47] S.B. Amor, G. Baud, J.P. Besse, and M. Jacquet. Structural and optical properties of sputtered Titania films. *Mat. Sci. Technol. B-Solid*, 47, 1997.
[48] Y. Leprince-Wang, D. Souche, K. Yu-Zhang, S. Fisson, G. Vuye, and J. Rivory. Relations between the optical properties and the microstructure of TiO2 thin films prepared by ion-assisted deposition. *Thin Sol. Films*, 359, 2000.
[49] D. Mergel, D. Buschendorf, S. Eggert, R. Grammes, and B. Samset. Density and refractive index of TiO2 films prepared by reactive evaporation. *Thin Sol. Films*, 371, 2000.
[50] Y. Yamada, H. Uyama, T. Murata, and H. Nozoye. Low temperature deposition of titanium-oxide films with high refractive indices by oxygen-radical beam assisted evaporation combined with ion beams. *J. Vac. Sci. Technol. A*, 19, 2001.
[51] M. Nakamura, S. Kato, T. Aoki, L. Sirghi, and Y. Hatanaka. Formation mechanism for TiOx thin film obtained by remote plasma enhanced chemical vapor deposition in H-2-O-2 mixture gas plasma. *Thin Sol. Films*, 401, 2001.
[52] Z.W. Zhao, B.K. Tay, and G.Q. Yu. Room-temperature deposition of amorphous titanium dioxide thin film with high refractive index by a filtered cathodic vacuum arc technique. *Appl. Optics*, 43, 2004.
[53] L.-J. Meng, V. Teixeira, H.N. Cui, F. Placido, Z. Xu, and M. Pereira dos Santos. A study of the optical properties of titanium oxide films prepared by dc reactive magnetron sputtering. *Appl. Surf. Sci.*, 252, 2006.
[54] C. Toccafondi, S. Uttiya, O. Cavalleri, G. Gemme, E. Barborini, F. Bisio, and M. Canepa. Optical properties of nanogranular and highly porous TiO2 thin films. *J. Phys. D*, 47, 2014.
[55] J. Aarik, A. Aidla, A.A. Kiisler, T. Uustare, and V. Sammelselg. Effect of crystal structure on optical properties of TiO2 films grown by atomic layer deposition. *Thin Sol. Films*, 305, 1997.
[56] H. Takikawa, T. Matsui, T. Sakakibara, A. Bendavid, and P.J. Martin. Properties of titanium oxide film prepared by reactive cathodic vacuum arc deposition. *Thin Sol. Films*, 348, 1999.
[57] M. Zhang, G. Lin, C. Dong, and L. Wen. Amorphous TiO2 films with high refractive index deposited by pulsed bias arc ion plating. *Surf. Coat. Technol.*, 201, 2007.
[58] M. Cevro and G. Carter. Ion-Beam sputtering and Dual-Ion-Beam sputtering of titanium-oxide films. *J.Phys. D*, 28, 1995.
[59] H. Demiryont and J. R. Sites. Effects of oxygen in ion beam sputter deposition of titanium oxides. *J. Vac. Sci.Technol. A: Vacuum, Surfaces, and Films*, 2, 1984.
[60] A. Bendavid, P.J. Martin, and H. Takikawa. Deposition and modification of titanium dioxide thin films by filtered arc deposition. *Thin*

Sol. Films, 360, 2000.
[61] C.R. Ottermann and K. Bange. Correlation between the density of TiO2 films and their properties. *Thin Sol. Films*, 286, 1996.
[62] Y.-J. Shi, R.-J. Zhang, H. Zheng, D.-H. Li, W. Wei, X. Chen, Y. Sun, Y.-F. Wei, H.-L. Lu, N. Dai, and L.-Y. Chen. Optical Constants and Band Gap Evolution with Phase Transition in Sub-20-nm-Thick TiO2 Films Prepared by ALD. *Nanoscale Res. Lett.*, 12, 2017.
[63] K.J. Hebert, S. Zafar, E.A. Irene, R. Kuehn, T.E. McCarthy, and E.K. Demirlioglu. Measurement of the refractive index of thin SiO2 films using tunneling current oscillations and ellipsometry. *Appl. Phys. Lett.*, 68, 1996.
[64] B.M. Ayupov, V.A. Gritsenko, H. Wong, and C.W. Kim. Accurate ellipsometric measurement of refractive index and thickness of ultrathin oxide film. *J. Electrochem. Soc.*, 153, 2006.
[65] J. Ehrstein, C. Richter, D. Chandler-Horowitz, E. Vogel, C. Young, S. Shah, D. Maher, B. Foran, P.Y. Hung, and A. Diebold. A comparison of thickness values for very thin SiO2 films by using ellipsometric, capacitance-voltage, and HRTEM measurements. *J. Electrochem. Soc.*, 153, 2006.